Astron. Astrophys. 318, 957–961 (1997)

ASTRONOMY AND ASTROPHYSICS

Heating of coronal holes by phase mixing

A.W. Hood, J. Ireland, and E.R. Priest

School of Mathematical and Computational Sciences, University of St. Andrews, St. Andrews, KY16 9SS, UK

Received 29 May 1996 / Accepted 22 July 1996

Abstract. A two-dimensional, analytical, self-similar solution to the Alfvén wave phase mixing equations is presented for a coronal hole model. The solution shows clearly that the damping of the waves with height follows the scaling predicted by Heyvaerts & Priest 1983 at low heights, before switching to an algebraic decay at large heights. The ohmic dissipation is calculated and it is shown that the maximum dissipation occurs at a height that scales with $\eta^{1/3}$. However, the total Ohmic dissipation is, of course, independent of the resistivity. Using realistic solar parameters it appears that phase mixing is a viable mechanism for heating the lower corona provided either the frequency of photospheric motions is sufficiently large or the background Alfvén velocity is sufficiently small.

Key words: MHD – waves – Sun: corona

1. Introduction

Phase mixing has been proposed as a means of efficiently dissipating Alfvén waves in the solar corona by Heyvaerts & Priest 1983, who suggested that shear Alfvén waves with amplitudes perpendicular to the background magnetic field would decay away with height above the basal excitation region.

Much work has been done on coronal heating by resonant absorption (Kappraff & Tataronis 1977; Ionson 1978; Hollweg 1987; Poedts & Kerner 1992; Ruderman & Goossens 1993; Goossens 1994; Karpen et al. 1994; Wright & Rickard 1995) but less on the related problem of phase-mixing (Browning & Priest 1984; Sakurai & Granik 1984; Nocera et al. 1984; Cally 1991).

Fig. 1 shows the basic model we are considering. Coronal holes can be modelled by this geometry, at least to a first approximation. The background Alfvén speed $v_A^2(x)$ is a function of x only and has gradients in the $\hat{x}$-direction. This inhomogeneity in the background field causes Alfvén waves on neighbouring field lines to have different wavelengths. Hence, as height increases, waves on neighbouring field lines move out of phase with each other, causing large gradients in the Alfvén wavefront, in the direction of the inhomogeneity. Dissipation then comes into play, allowing the energy in the wave to heat the plasma. Consider a wave equation for phase-mixing in a non-dissipative system, i.e.,

$$\frac{\partial^2 v}{\partial t^2} = v_A^2(x)\frac{\partial^2 v}{\partial z^2}. \tag{1}$$

The solution is

$$v \sim \exp\left[-i(\omega t + k(x)z)\right], \tag{2}$$

for a wave of frequency ω, where $k(x) = \omega/v_A(x)$. Note that,

$$\frac{\partial v}{\partial x} \sim v.z.k'(x), \tag{3}$$

i.e., gradients in the $x-$direction increase with height. The appearance of sharp gradients is also mediated by the gradient of $k(x)$. Hence large gradients in the Alfvén wavefront will appear at lower heights when the plasma is more inhomogeneous. It is these large gradients that will be substantially affected by the presence of dissipation in the plasma (see Sect. 3.2 and Figs. 5, 4).

Using the ansätz,

$$v \sim \hat{v}(x,z)\exp\left[-i(\omega t + k(x)z)\right] \tag{4}$$

and assumptions of *weak damping*,

$$\frac{1}{k}\frac{\partial}{\partial z} \ll 1 \tag{5}$$

and *strong phase mixing*,

$$\frac{z}{k}\frac{\partial k}{\partial x} \gg 1 \tag{6}$$

Heyvaerts & Priest obtained the form

$$\hat{v}(x,z) = \hat{v}(x,0)\exp\left[-\frac{1}{6}\left(\frac{k(x)z}{R_{Tot}^{1/3}}\right)^3\right] \tag{7}$$

for the velocity, where

$$R_{Tot} = \frac{\omega}{\eta+\nu}\left(\frac{d}{dx}\log k(x)\right)^2 \tag{8}$$

Send offprint requests to: A.W. Hood

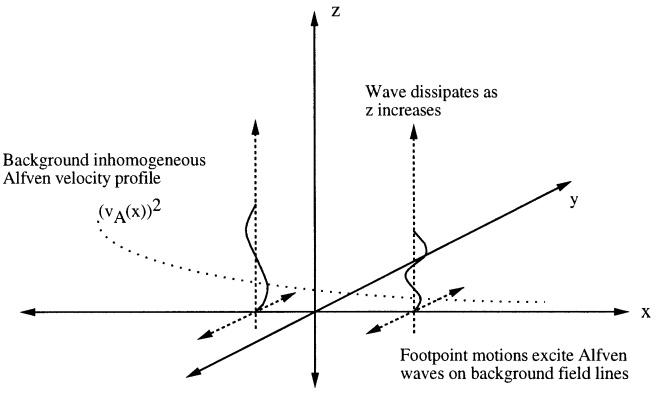

Fig. 1. Heyvaerts & Priest 1983 model of phase mixing.

and η is the magnetic diffusivity and ν is the kinematic viscosity.

The main feature to note is the $\exp(-z^3)$ decay with height, which indicates a strong decay for a large enough height. However, this solution is only valid under the conditions described above. In particular, it is not valid at small z where it breaks condition 6. Nonetheless, the decay is fast enough to warrant further investigation to see under what conditions it can be reproduced.

2. Basic equations

The simplest model of phase mixing consists of a vertical magnetic field with the photospheric footpoints being oscillated at frequency ω. If the Alfvén speed is non-uniform in the horizontal direction, then the waves generated at the footpoints propagate with different wave speeds and soon become out of phase. Large horizontal gradients are created and dissipation can then damp the waves and release their energy.

Thus, we assume the equilibrium is

$$\mathbf{B}_0 = (0, 0, B_0),\ \rho_0 = \rho_0(x), \tag{9}$$

and consider a perturbation of the velocity and magnetic field in the $y-$direction only so that phase mixing of Alfvén waves is produced. Hence, the linearised MHD equations are

$$\rho_0 \frac{\partial v}{\partial t} = \frac{B_0}{\mu}\frac{\partial B}{\partial z}, \tag{10}$$

and

$$\frac{\partial B}{\partial t} = B_0 \frac{\partial v}{\partial z} + \eta \nabla^2 B, \tag{11}$$

for the perturbed velocity, v, and magnetic field B. These equations can be combined to give (see Heyvaerts & Priest 1983)

$$\frac{\partial^2 B}{\partial t^2} = v_A^2(x)\frac{\partial^2 B}{\partial z^2} + \eta\left(\frac{\partial^2}{\partial x^2} + \frac{\partial^2}{\partial z^2}\right)\frac{\partial B}{\partial t}, \tag{12}$$

where $v_A^2(x) = B_0^2/[\mu\rho(x)]$ is the Alfvén speed squared. The important terms for phase mixing are the first and second terms on the right-hand side of (12). The first term indicates that the wavelength is different on each field line and this generates the large horizontal gradients that are damped by the second term. The last term in (12) is not important for phase mixing and will be neglected from now on.

A simple self-similar solution is presented in the next section that allows us to investigate the efficiency of phase mixing as a mechanism for heating coronal holes.

3. Similarity solution

A self-similar solution can be found for the particular Alfvén speed profile

$$v_A^2(x) = v_{A0}^2 e^{-2x/a}. \tag{13}$$

Set

$$B(x, z, t) = F(s)e^{i\omega t}, \tag{14}$$

where the self-similar variable is

$$s = e^{x/a} z/H. \tag{15}$$

Choosing the vertical lengthscale as $H = v_{A0}/\omega$ and defining

$$\delta = \eta/a^2\omega, \tag{16}$$

the dimensionless form of (12) reduces to

$$(1 + i\delta s^2)\frac{d^2F}{ds^2} + i\delta s\frac{dF}{ds} + F = 0, \tag{17}$$

which may be rewritten as

$$(1 + i\delta s^2)^{1/2}\frac{d}{ds}\left((1 + i\delta s^2)^{1/2}\frac{dF}{ds}\right) + F = 0. \tag{18}$$

This may be expressed in terms of a new independent variable w as

$$\frac{d^2F}{dw^2} + F = 0, \tag{19}$$

where w is related to s by

$$\frac{ds}{dw} = (1 + i\delta s^2)^{1/2}. \tag{20}$$

The boundary conditions are taken as

$$F(0) = 1 \text{ and } F \to 0 \text{ as } s \to \infty. \tag{21}$$

Thus, we are modelling the generation of waves with no preferred wavelength at the base that are outward propagating and damped at large heights. The similarity variable s can simply be thought of as height, since the equation of the field lines is x a constant so that s is linearly proportional to z.

Before considering the exact solution to (17) we consider a couple of special cases. For $\delta s^2 \ll 1$ the solution to (17) is approximately

$$F \approx e^{-is}, \tag{22}$$

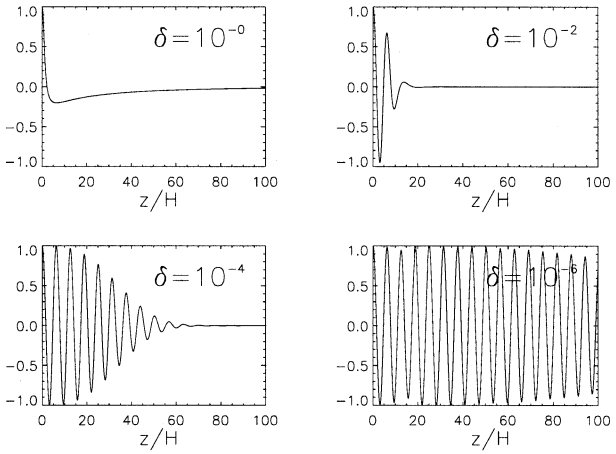

Fig. 2. The real part of the perturbed magnetic field as a function of height (z) for various values of δ.

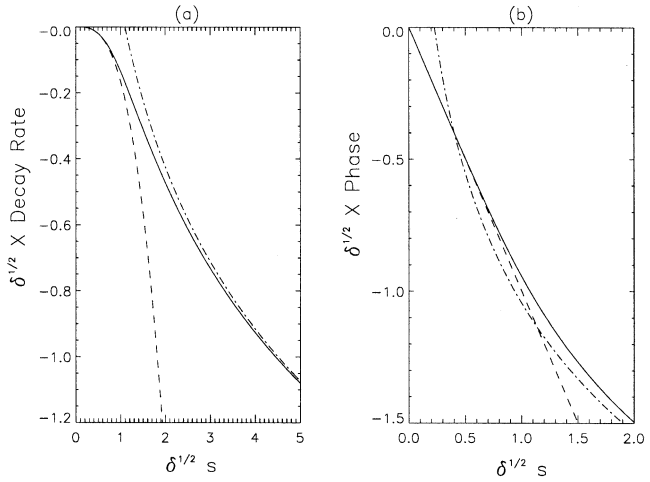

Fig. 3. a The real part of the exponent in (25) (solid line), scaled with respect to $\delta^{1/2}$, is shown as a function of $\delta^{1/2}s$. The dashed curve refers to (28) and the dot-dashed curve to (29). **b** The corresponding phase of the exponent (solid curve), scaled with respect to $\delta^{1/2}$, is shown as a function of $\delta^{1/2}s$. The dashed curve refers to the imaginary part of the exponent in (26) and the dot-dashed curve refers to (35)

whereas for $\delta s^2 \gg 1$ it is

$$F \approx \left((i\delta)^{1/2}s\right)^{-n}, \tag{23}$$

with $n = (i/\delta)^{1/2}$.

Finally, the height at which the solution switches from (22) to (23) is controlled by the size of δ and is approximately given by

$$s \approx \delta^{-1/2}. \tag{24}$$

The exact solution to (17) that satisfies the boundary conditions (21) is

$$F(s) = \exp\left(-(\frac{i}{\delta})^{1/2}\log\left[(i\delta)^{1/2}s + (1+i\delta s^2)^{1/2}\right]\right). \tag{25}$$

The branches of the square roots are defined by taking $\sqrt{1} = 1$ and the logarithmic function by $\log(1) = 0$. The real part of the solution is plotted in Fig. 2 as a function of height for the particular field line given by $x = 0$. For small enough values of δ (e.g. $\delta = 10^{-6}$) it is clear that the solution simply oscillates with very little damping evident at these heights. However, $\delta = 10^{-2}$ shows strong damping with little oscillation. Finally, $\delta = 1$ has fast damping with no oscillations. These different types of solution can be understood by examining the real and imaginary parts of the exponent in (25).

3.1. $\delta s^2 \ll 1$ *and* $\delta s^2 \gg 1$

Consider the case $\delta s^2 \ll 1$. The exponent in (25) may be expanded to give

$$F(s) = \exp(-is - \delta s^3/6). \tag{26}$$

This shows that the basic Alfvén wave is only exponentially damped when δs^3 is of order unity. There is minimal damping if δs^3 is small. This form of the damping is in agreement with the results of Heyvaerts & Priest 1983. Thus, there is a "window" in height for which the wave is damped before the weaker algebraic damping of (23) takes over. This window is given by

$$\delta^{-1/3} < s < \delta^{-1/2}. \tag{27}$$

Within this region the wave amplitude will decay by an amount $\exp(-1/\delta^{1/2})$. So the smaller the value of δ the more the wave is damped but the further the wave travels before damping sets in.

The way the wave damps can be investigated by studying the real part of the exponent of (25). For $\delta s^2 \ll 1$ the damping is given by (26), namely,

$$-\delta s^3/6, \tag{28}$$

and for $\delta s^2 \gg 1$ by

$$\frac{1}{(2\delta)^{1/2}}\left[\frac{\pi}{4} - \log(2\delta^{1/2}s)\right]. \tag{29}$$

The real part of the exponent is shown in Fig. 3a together with the approximations (28) and (29). The variation of the phase is given by the imaginary part of the exponent in Eq. (25) and is shown in Fig. 3b. Since the phase is not simply the straight line $-s$, this means that the wavefronts will turn with height, as discussed in the next section.

We now interpret these results in terms of the assumptions of weak damping and strong phase mixing. The definitions given by Heyvaerts & Priest 1983 and in Sect. 1 are limited by their choice of ansätz and were used to simplify the equations. Weak damping means that the wave propagates for many periods before significant damping occurs. Thus, by expressing the perturbed magnetic field in the form

$$\exp\{-D(x,z) + iP(x,z)\}, \tag{30}$$

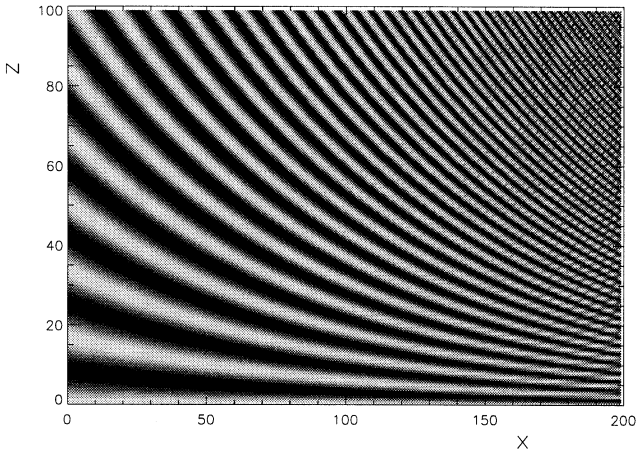

Fig. 4. Contour plot of the real part of the Alfvén wave profile for Eq. 1 in the absence of damping, $\delta = 0$. Lighter shades of grey correspond to higher values of $Re\,(F(s))$, darker shades to lower values of $Re\,(F(s))$.

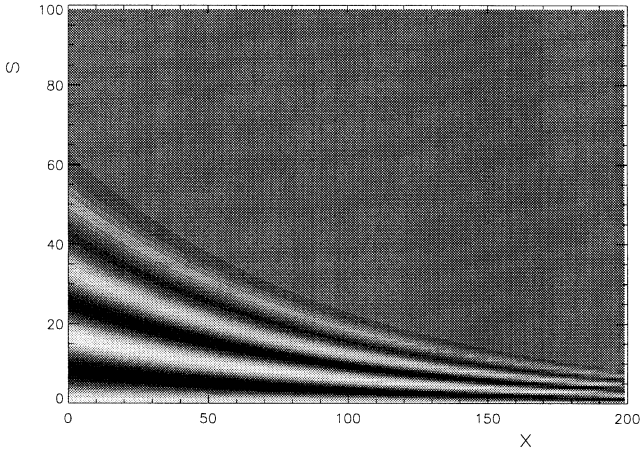

Fig. 5. Contour plot of the real part of the Alfvén wave profile for $\delta = 10^{-3}$. Lighter shades of grey correspond to higher values of $Re\,(F(s))$, darker shades to lower values of $Re\,(F(s))$.

where $-D(x,z)$ and $P(x,z)$ are the real and imaginary parts of the exponent in (25), weak damping can then be interpreted as

$$\frac{\partial D}{\partial z} \ll \frac{\partial P}{\partial z}. \tag{31}$$

Hence, weak damping occurs only when

$$\delta s^2 \ll 1. \tag{32}$$

Strong phase mixing means that the horizontal length-scales are much shorter than the vertical length-scales, so that

$$\frac{\partial B}{\partial x} \gg \frac{\partial B}{\partial z}. \tag{33}$$

This reduces to

$$z \gg a, \tag{34}$$

so that strong phase mixing occurs above heights corresponding to the horizontal inhomogeneity length.

3.2. Wave turning

As was mentioned in Sect. 1, the inhomogeneity in the background Alfvén speed causes Alfvén waves on neighbouring field lines to move out of phase with each other. Hence, as the wave progresses in z, the wavefront will turn consistent with the background inhomogeneity. One can view the creation of shorter lengthscales in the plasma as a result of wavefront turning. Fig. 4 shows the real part of the self-similar solution to the non-dissipative Eq. 1 in contour form, with initial condition $F(0) = 1$. As z increases, the number of wavefronts crossing the line $z = constant$ increases. Therefore, cross-sections along the $x-$direction show far more structure due to the appearance of gradients. These gradients can be dissipated, as is shown in Figs. 5 and 6 (plotted using Eq. 25 with $\delta = 10^{-3}$ and $F(0) = 1$).

Fig. 6 shows a surface plot of the Alfvén wave profile. Starting from a disturbance that is uniform in x at $z = 0$, the surface plot clearly shows the rapid generation of short length-scales in the x-direction: the shorter these length-scales are, the faster the wave damps.

As can be seen, Fig. 5 has far less fine structure than Fig. 4, due to dissipation at high values of z, and so the increased wave turning in Fig. 5 is not visible.

The non-dissipative Eq. 1, has self-similar solution $\exp(-is)$, which has the same phase as Eq. 26, obtained under the assumption $\delta s^2 \ll 1$. The equation for the position of the wavefront is simply $z = c\exp(-x/a)$ for some $c > 0$. In the limit $\delta s^2 \gg 1$, the phase is given by

$$\frac{-1}{(2\delta)^{1/2}}\left[\frac{\pi}{4} + \log(2\delta^{1/2}s)\right]. \tag{35}$$

Fig. 3b demonstrates the behaviour of the phase of the solution with increasing $\delta^{1/2}s$. The phase in this limit is advanced with respect to the non-dissipative solution.

3.3. Ohmic dissipation

The earlier discussion has shown that the wave amplitude is decaying with height. The energy of the wave is transferred into heat through ohmic dissipation. The analytical solution for the perturbed magnetic field allows the current and ohmic dissipation to be calculated. Assuming $x = 0$, so that $s = z/H$, the ohmic dissipation is

$$\frac{j^2}{\sigma} = \eta\frac{\left(\frac{a^2}{H^2} + s^2\right)|B|^2}{\sqrt{1+\delta^2 s^4}}. \tag{36}$$

The modulus of B can be estimated using the approximation (26) and $s \gg 1$ so that

$$\frac{j^2}{\sigma} \approx \eta s^2 e^{-\delta s^3/3}. \tag{37}$$

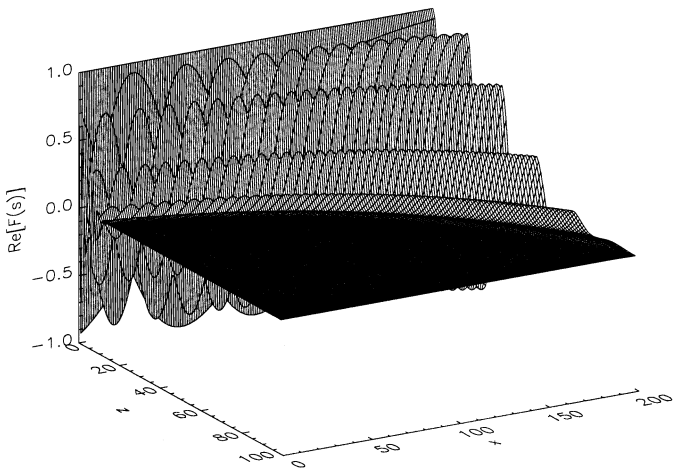

Fig. 6. Surface plot of the Alfvén wave profile for $\delta = 10^{-3}$.

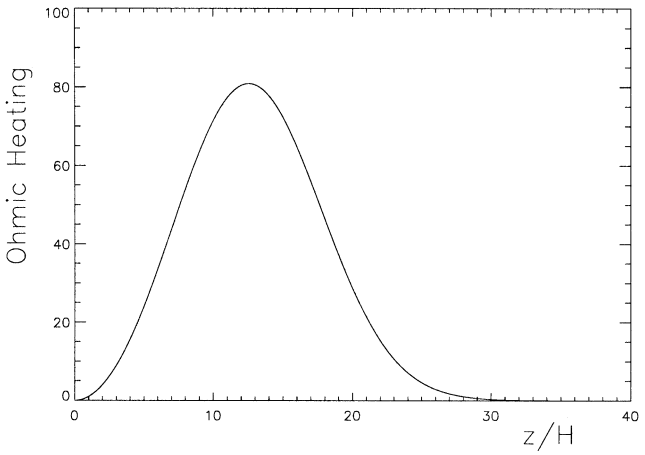

Fig. 7. The ohmic dissipation, in arbitrary units, as a function of height for $\delta = 10^{-8}$.

The exact ohmic dissipation and the approximation (37) are plotted in Fig. 7. The curves lie almost on top of each other for $\delta = 10^{-8}$. Using (37), the location and the value of the maximum dissipation can be estimated as

$$s_{max} \approx \left(\frac{2}{\delta}\right)^{1/3} \tag{38}$$

and

$$\left[\frac{j^2}{\sigma}\right]_{max} \approx \eta \left(\frac{2}{\delta e}\right)^{2/3}. \tag{39}$$

For this value of s_{max} to be valid we must make sure that $\delta s_{max}^2 \ll 1$, which is ensured by having $(4\delta)^{1/3} \ll 1$.

Obviously there is also the magnitude of the wave amplitude still to be included. However, using the definition of $\delta = \eta/\left(a^2\omega\right)$, the maximum ohmic dissipation scales as

$$\eta^{1/3}\omega^{2/3}a^{4/3}. \tag{40}$$

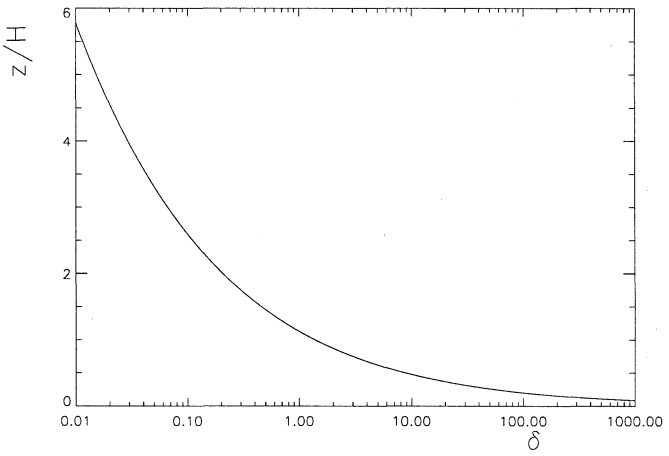

Fig. 8. Height (z) of the maximum ohmic heating as a function of $\delta = \eta/\left(a^2\omega\right)$, expressed in units of H. This has been calculated using the full expression for $F(s)$, Eq. 25.

Thus, the amount of coronal heating by phase mixing depends on the frequency and the phase mixing length as well as the resistivity.

Finally, the total amount of Ohmic heating can be estimated by integrating (37) over height to give

$$\int_0^\infty \frac{j^2}{\sigma} dz \approx \frac{\eta}{\delta} = a^2\omega. \tag{41}$$

Thus, the total Ohmic dissipation is independent of resistivity, as one would expect but it does depend on the phase mixing length and the wave frequency.

4. Discussion

We have here discovered a two-dimensional, self-similar solution for phase mixing in an inhomogeneous magnetic field. It depends on a parameter, δ, which can be written as

$$\delta = \frac{1}{S}\left(\frac{A}{a}\right)^2, \tag{42}$$

where the Lundquist number, $S = A^2\omega/\eta$, A is the size of the coronal hole region and a is the lengthscale of the plasma inhomogeneity. The parameter δ, therefore, combines the relative strengths of phase mixing (through the value of (A/a) and dissipation (through the Lundquist number S).

Using this solution, we have verified that an $\exp(-z^3)$ height-dependence does exist, as predicted by Heyvaerts & Priest 1983, over a height range given by

$$\delta^{-1/3} < s < \delta^{-1/2}. \tag{43}$$

Fig. 8 shows that the height of maximum dissipation depends on the value of δ and therefore on the values of a, η and ω, all of which are highly uncertain: the dissipation height decreases with both a and ω.

Consider the following example. For $\omega = 2\pi/300s^{-1}$ and $v_A = 4.5 \times 10^6 ms^{-1}$ (corresponding to a high speed solar wind blowing from a coronal hole) we require $10^{-3} \lesssim \delta \lesssim 1$ to place the maximum ohmic heating in the range $0.3R_\odot \lesssim z_{max} \lesssim 4R_\odot$. With these values, the wave dissipates within a few wavelengths H which agrees with Heyvaerts & Priest.

Limits on δ can also be used to place limits on the Lundquist number S and inhomogeneity lengthscale a. For a coronal hole size $A \sim 10^8 m$ (Ofman & Davila 1995) we obtain

$$10^{16}m^2 \lesssim a^2 S \lesssim 10^{19}m^2 \quad (44)$$

If we further assume that at worst $a \sim A$ and at best $a \sim 10^3 m$ (Woo 1996) then $1 \lesssim S \lesssim 10^{13}$: this implies that we can dissipate Alfvén waves at reasonable heights in the corona over a wide range of possible Lundquist number, given a particular inhomogeneity scale. If either the background Alfvén speed v_A or the period of the phase-mixed Alfvén wave is reduced, H decreases, allowing more oscillations and hence more phase mixing to occur for a given height. For a fixed Lundquist number this implies that the wave will be dissipated at a lower height.

It should be noted that Alfvén waves with periods about $\sim 300s$ and wavelengths on the order of $10^5 km$ should be observable by the CDS (Coronal Diagnostic Spectrometer) instrument on board the recently launched SoHO (Solar and Heliospheric Observatory) platform and that studies are in place to look for Alfvén waves in coronal holes (Harrison and Hassler 1995). Future theoretical work will concentrate on similar phase-mixing equations for different background Alfvén speed structures.

Acknowledgements. J. Ireland wishes to thank PPARC for financial support.

References

Browning, P.K., Priest, E.R. 1984, Kelvin-Helmholtz instability of a phase-mixed Alfvén wave, Astron. Astrophys., 131, 283

Cally, P.S. 1991, Phase mixing and surface waves: a new interpretation, J. Plasma Phys., 45, 453

Goossens, M. 1994, Alfvén wave heating, Space Sci. Rev., 68, 51

Harrison, R.A., Hassler, D. 1995, Enhanced line broadening with altitude -[BROAD], The coronal diagnostic spectrometer for the solar and heliospheric observatory: scientific report, edited by R.A. Harrison and A. Fludra, August 1995

Heyvaerts, J. Priest, E.R. 1983, Coronal heating by phase mixed shear Alfvén waves, Astron. Astrophys., 117, 220

Hollweg, J.V. 1987, Resonance absorption of magnetohydrodynamic surface waves: physical discussion, Astrophys. J., 312, 880

Ionson, J.A. 1978, Resonant absorption of Alfvénic surface waves and the heating of coronal loops, Astrophys. J., 226, 650

Kappraff, J.M., Tataronis, J.A. 1977, Resistive effects on Alfvén wave heating, J. Plasma Phys., 182, 209

Karpen, J.T., Dahlburg, R.B., Davila, J.M. 1994, The effects of Kelvin-helmholtz instability on resonance absorption layers in coronal loops, Astrophys. J., 421, 372

Nocera, L., Leroy, B., Priest, E.R. 1984, Phase-mixing of propagating Alfvén waves, Astron. Astrophys., 133, 387

Ofman, L., Davila, J.M. 1995, Alfvén wave heating of coronal holes and the relation to the high speed solar wind, J. Geophys. Res., 100, A12, 23413

Poedts S., Kerner, W. 1992, Time scales and efficiency of resonant absorption in periodically driven resistive plasmas, J. Plasma Phys., 471, 139

Ruderman, M.S., Goossens, M. 1993, Nonlinearity effects on resonant absorption of surface Alfvén waves in incompressible plasmas, Solar Phys., 143, 69

Sakurai, T., Granik, A. 1984, Generation of coronal electric currents due to convective motions on the photosphere. II. Resonance and phase mixing due to Alfvén waves, Astrophys. J., 177, 404

Woo, R. 1996, Kilometre-scale structures in the Sun's corona, Nature, 379, 321

Wright, A.N., Rickard, G.J. 1995, A numerical study of resonant absorption in a magnetohydrodynamic cavity driven by a broadband spectrum, Astrophys. J., 444, 458

This article was processed by the author using Springer-Verlag LaTeX A&A style file *L-AA* version 3.